Simulation of Light Field Fundus Photography

Sha Tong
Stanford University
shat@stanford.edu

T.J. Melanson
Stanford University
melanson@stanford.edu

Abstract

The light field camera, due to its capability to computationally perform flexible image manipulation such as digital refocusing and view point shift, have potential to enable some unique applications in the medical imaging field, where most objectives are intrinsically three dimensional. In this study, we explored the feasibility of using light field camera to record the image of the human retina (fundus). We designed a simple light field fundus camera that includes a Gullstrand eye model and a generic light field camera. We developed a ray tracing tool in Matlab to help us to simulate the image formation in such system. The results are then compared to the simulated image obtained using traditional camera. We concluded that despite many challenges, light field camera has potential to simplify the traditional fundus camera design and provide better performance. .

1. Introduction

1.1. Motivation

Retinal imaging is important in the diagnosis and monitoring of retinal health. A fundus camera is a complex optical system that makes use of the principle of reflex free indirect ophthalmoscopy to image the retina [1]. Imaging the retina presents a unique design challenge for a number of reasons. A few important ones are (1) Low signal to noise ratio. The retina is not directly accessible because it is located at the posterior of the eye. To image the retina in a noninvasive manner the retina must be illuminated and imaged simultaneously [2]. The retina itself is a minimally reflectively and highly scattering surface [3-4]. which requires imaging and illumination optical path need to be spatially separated and all sources of ghost reflections and stray light in the imaging path need to be identified and eliminated. (2) Limited field of view. Since retinal imaging conjugates the near spherical retina to planar camera sensor, the camera field of view is usually limited to about 30 degree due to tradeoff between field of view and depth of focus. (3) Inherent optical aberration inside the system. Imaging the retina inherently includes the optics of the eye in the imaging path. As a result, any device used for retina imaging in the mass population must be able to accommodate for the large source of optical aberrations such as refractive error, defocusing and astigmatism.

Light field camera, as described by Ren Ng, etc [5], has been a popular research topic in the computational image field. The fact it can simultaneously recording location and angle allows researchers to discover some interesting applications such as glare and reflection removal [6], digital refocusing [5] and aberration correction [7]. These unique capabilities may address some of the challenges facing normal camera in retina imaging mentioned above and provide performance or cost advantages.

1.2. Related Work

So far we discovered very limited studies conducted in this specific application. One patent application submitted by Carl Zeiss Corporation in 2012 proposed the idea of using light field camera for fundus photography and discussed the potential benefits [8]. Turola and Gruppetta proposed to study the 4D light field retina imaging through numerical simulation [9]. A group from UVEG showed some experimental setup on Plenoptic Fundus Camera [10]. We also discovered Wills Eye started fundus Plenoptic photography clinical study in February of 2017. The purpose is to establish the quality of fundus images produced by Lytro camera [11], indicating continue commercial interest of such device in the industry. Unfortunately, detailed information of such study is not disclosed.

2. Camera Design

Fig 1 illustrates our camera optical design. The system consists of a Gullstrand's eyeball model [12] and a generic light field camera. Gullstrand's 4 radius model is well-known and can be described as paraxial models which works well for small aperture sizes and small field angles. Use retina as the objective, any point on retina will be imaged by eye lens at near infinite and each ray bundle (as

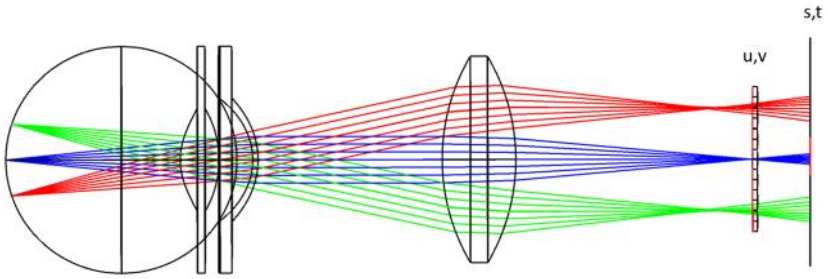

Figure 1: Light Field Funds Camera Design.

illustrated by different colors) has the same cross dimensions as pupil as it exits the eye ball. The camera's main imaging lens is placed at the location that is one focal length $f_{main} = 24mm$ away from the principal plane of the eye lens. The imaging lens is assumed as a perfect lens that is free of aberrations except field curvature. As a result, instead of focusing on a plane, the ray bundles will be focused on a spherical surface with radius of curvature linearly proportional to focal length of the imaging lens. This implies the sharp image can only obtained in a limited area if a 2D sensor is placed at the focal plane. This problem was studied by O. Pomerantzeff, etc. [13] where he purposed different methods to optically correct the curvature and make images of retina points coplanar.

The micro lens array is placed at focal length f_{main} behind the imaging lens and the sensor array is placed behind the micro lens array with distance equal to the focal length of the micro lens $f_{micro} = 40\mu m$. Each micro lens has diameter $20\mu m$ and the size of the array is 600 by 600, which is the maximum resolution the camera will support. Micro lens and main imaging lens has matched numerical aperture $NA = 0.5$. Each sensor has pixel size $1\mu m$ and therefore there is a 20 by 20 sensor array behind each micro lens. Use the light field representation proposed by Levoy [14]. By define micro lens array as (u, v) plane and sensor as (s, t) plane. The 4D light field is captured by recording the coordinates on both (u, v) and (s, t) planes for each ray under consideration.

Traditional camera can be simply implemented by directly replacing the micro lens array with sensor array at the same location.

3. System Numerical Implementation

3.1. System Implementation

Given the novelty of the light field application, and therefore the smaller number of physical resources to accomplish the task, the majority of the experiment was conducted via simulation. Rather than taking physical images of the camera, then adjusting the lenses as needed, the subject, light source, and camera lenses were simulated through a raytracer. This allows easy manipulation of current lenses, as well as the addition and resizing of new lenses.

3.2. Spherical Mapping

Because a physical subject would not be available for the Matlab simulation, there needed to be an alternative to the physical fundus. For this situation, we used a 2-D image of the fundus (500pix X 500pix), obtained by special imaging, as a "ground truth" for how the fundus camera would appear mapped from spherical to planar curvature. Then, the given 2-D image was converted from a planar image into a spherical point system via a simple spherical equation $z^2 = R^2 - x^2 - y^2$, where R is the radius of the sphere, x and y are determined from the location of the pixel along the image (i.e. a (u,v) pixel location translated into world coordinates), and the output z is the determined depth location of the resulting pixel coordinate.

For the given result, we found that the fundus image was high enough resolution that a mapping of the pixels onto a curved surface could best approximate a spherical fundus. Additionally, the image location in the back of the eye was planar enough that the features on the 2-D image were not warped by the spherical mapping.

3.3. Raytracing

In order to simulate the fundus light field camera, rather than physically manipulate the lens parameters, a raytracing application was built using a combination of Matlab and Zemax. The ray tracer first traces light came from an image source, mapped onto a spherical curvature. Gullstrand's eyeball model is then simulated using Zemax to compute the exiting angle of rays originated from retina. After exiting from the eye, the ray keep propagating through main lens and micro lens and changes angle twice before it arrives on sensor. These steps are simulated as transformations of the

incident rays via Matlab. The output was recorded from the intensity at the light field sensor. Through this model, every ray originated from retina will be mapped to a single point on the sensor array as illustrated in Fig 2.

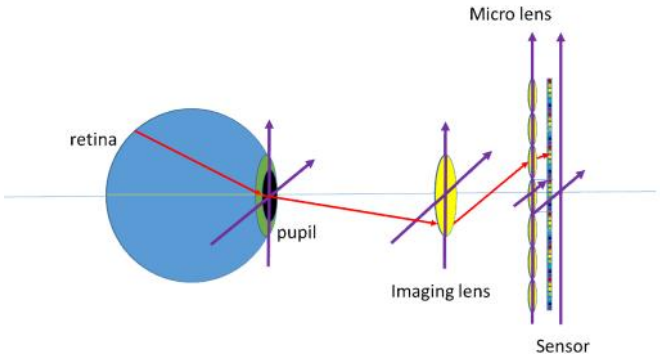

Fig 2 illustrates the optical path of single ray from objective to sensor.

3.4. Retina Imaged by Eye Lens

In order to naturally represent a fundus image, there needed to be an accurate way to convert the rays coming from a retina to the rays entering the imaging lens. The complexity is due to the fact that angle transformation of the 4 surfaces eye lens is an un-linear function of retina location. We therefore decided to use Zemax's "eye objective" model [15] to simulate this process. The model traces the light as it propagated from the retina through the eye lens and the pupil, stored as a series of rays with exiting angles.

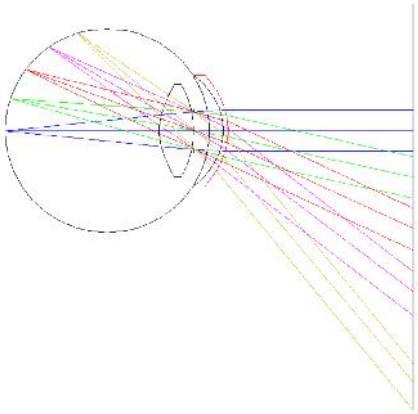

Fig 3: Zemax ray tracing of retina as objective, imaged by eye lens

3.5. Ray Tracing in Light Field Camera

Once the incidence ray is established, it is then read and processed by the "light field" camera simulated in Matlab. The raytracing application turns the rays into a 4 DOF line: vertical position *x*, horizontal position *y*, vertical angleβ, and horizontal angleθ. The transformation of angle and position is implemented by using *ABCD* ray transfer matrix method as follows:

$$\begin{pmatrix} x_2 \\ \theta_2 \end{pmatrix} = \begin{pmatrix} A & B \\ C & D \end{pmatrix} \begin{pmatrix} x_1 \\ \theta_1 \end{pmatrix},$$

Where x_1 and θ_1 are incidence angle and position and x_2 and θ_2 are exit angle and position.

The large imaging lens is discretized into a 2D grid as illustrated in Fig 4 representing different part on the lens. The numbers of total grid represent the total numbers of rays traced for a single pixel in the simulation. For our study, we fixed this number at 1000.

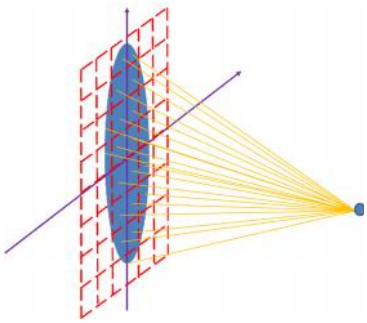

Fig 4: Discretizing of the lens

The image at the sensor is recorded as the sum of the ray intensities at each pixel. The ray intensity is determined both by the strength of the original pixel/source and the angle of incidence at that area. The results are stored in a 5D matrix (micro lens pixel x, micro lens pixel y, sensor pixel x, sensor pixel y and color) representing the recorded light field.

3.6. Processing of Light Field Images

After the image was collected, the resulting image had to be processed to accomplish two goals: first, to denoise the errors in the image caused by discretization; second, to analyze the result of the light field for an all-in-focus image as well as a depth map for possible 3-D reconstruction.

In a lot of the first iterations of the output image, a gridding pattern emerged due to the precision limit of the raytracing process. In order to counter this, besides high density ray tracing, a median filter was used to clean up the image.

One major advantage of recording the light field is the ability to retrieve several photos of the same subject from several different viewpoints, especially since those viewpoints are evenly spaced. Because of this, by using "shift and add" method [16], a set of images that focus the objective at different distance can be generated, which is known as "focal stack".

In order to create the all-in-focus image, the discrete derivatives of each of the images were taken. Then, the

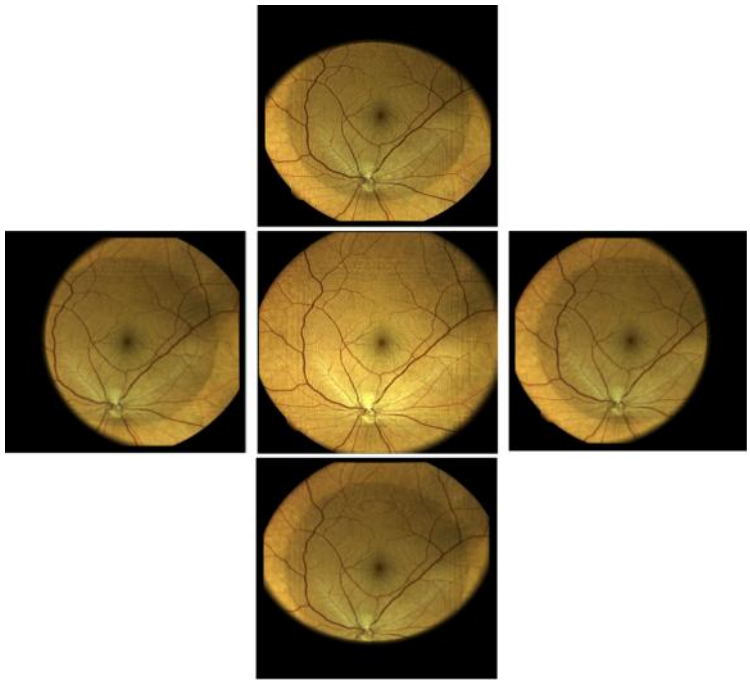

Fig 6: Light Field Images from Different Viewing Points

Fig 7: Focal Stack

images were combined such that the sharpest pixel (highest derivative at the point) in each stack was chosen in the final image.

The location of each pixel in the stack could also be used as a pseudo-depth variable. Because of this, the derivative map of the all-in-focus image can be combined with this depth variable to form a depth image. The depth image, as well as the all-in-focus image, is displayed in the results below.

(a) (b)

Fig 5: Fundus Image formed on Regular Camera
(a) $fc = f_{main}$ (b) $fc = 0.8 * f_{main}$

4. Results and Discussions

4.1. Fundus Imaging using Regular Camera

First, we simulate the normal camera image formation under different magnitude of the field of curvature. Two different cases were simulated: field of curvature equal to focal length of the main lens $fc = f_{main}$ and field of curvature less than the focal length of the main lens $fc = 0.8 * f_{main}$. The results are illustrated in Fig 5. As expected, due to the presence of the field of curvature, only the center part of the retina can be recorded clearly and outside image is blurred. For the image with the fixed size, the situation becomes worse as the radius of curvature decreases. Same $fc = 0.8 * f_{main}$ was used in the light field camera simulation.

4.2. Fundus Imaging using Light Field Camera

Fig 6 shows the light field images from different viewing points. Our camera has a 20X20 sensor array behind each micro lens allowing 400 different viewing points. The center view correspond to viewing directly into the eye through the center of the pupil at the normal angle as illustrated by the blue rays in Fig 1. This is the only viewing point produces the perfect circle apertured image by the pupil. The side views corresponds to viewing into the retina through the pupil with an angle so part of the view is blocked by pupil. Also, it is worth to notice the pictures for different view point are already all in focus since in this particular configuration, picking the corresponding pixel after each micro lens is equivalent as picking the rays from

Fig 9: Comparisons between normal camera (L), light field camera (M) and reference image (R)

each ray bundle and spatially resolving these bundles.

Fig 7 shows the exemplary images of the focal stack generated. Three pictures from top to bottom shows center focus, middle focus and edge focus.

Fig 8 shows the all focus image generated through focal stack and also the corresponding depth map expressed in HSV format. The center of the depth map has some noticeable grid like features which is caused by unequal space between image pixel and sensor pixel. This problem can be fixed by using method to allow more continuous coverage of image on sensor array such as using ray with finite size instead of infinitesimally small.

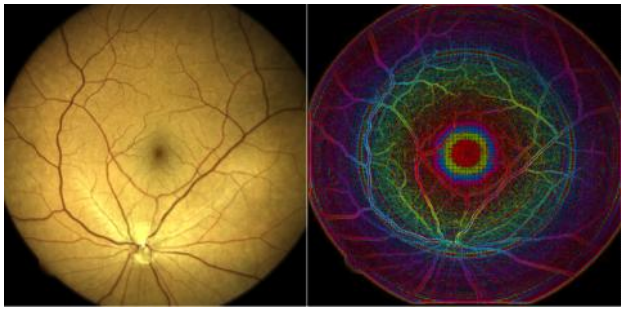

Fig 8: All in focus picture from focal stack and depth map

Finally, in Fig 9, we compared image quality of light field camera and normal camera to our reference image. The reference image has 500pixX500pix resolution and since the light field camera we simulate has 600X600 lens array, there is no loss of resolution. If the reference has higher pixel value than 600X600, loss of resolution would occur. The image of the light field camera appears having the same image quality as the original one while the image obtained by normal camera is mostly blur.

5. Conclusions and Discussion

In this study, through simulation, we demonstrated the light field camera has potential to simply the traditional fundus camera design and provide better performance. The study, however, is only limited to a small aspect of the challenges facing fundus imaging, specifically, field of curvature in lens aberration. More studies therefore are required in order to completely evaluate its potentials. The concept, on the other hand, is also relatively new so better techniques are expected to be continuously developed and adopted in the future.

One aspect worth to explore in the future is the noise reduce techniques. As fundus camera is very sensitive to optical noise such as reflection from other surface, large effects are put into system design to ensure the elimination of any reflection, glare and ghost image. Light field camera may provide large leverage in this particular aspect if noise can be completely removed by computational means. This could leads to dramatically reduction in system complexity.

Other optical aberrations such as coma, astigmatism and refractive errors are not included in our study. In reality, these aberrations exist simultaneously and are corrected by complicated optical design. It would be necessary to study further on both techniques and performance of using light field camera to correct these aberrations.

Another area light field may have advantage is the stereoscopic images generation, which is typically done by taking two pictures from different viewing point. With the light field camera, it is possible to generate one shot stereoscopic images using images from different viewing points.

Resolution wise, typical fundus camera has resolution about 4M~6M pixel, which is approximately the same as the resolution provided by Lyto II. Higher resolution ewill likely requirement would likely impose challenge for the light field camera.

Our ray tracing model does a reasonably well just to simulate the image formation. But he center image still is prone to noise, as it has the greatest concentration of incoming noise. A major improvement would be to successfully denoise the center image, either by selective Gaussian blurring or by another means. Additionally, there could be a better measurement of the subject plane, as the current spherical mapping could be prone to spherical warping. Using an actual light capture from a fundus camera could provide more useful for testing the light field camera.

References

[1] E.A. Dehoog. Noval Fundus Camera Design, 2008

[2] F. C. Delori and K. P. Pflibsen, "Spectral reflectance of the human ocular fundus," Appl. Opt. **28**, 1065-1077 (1989).

[3] M. Hammer and D. Schweitzer, "Quantitative reflection spectroscopy at the human," Phys. Med. Biol. **47**, 179-191 (2002).

[4] T. E. Choe, etc, "2-D registration and 3-D shape inference of the Retinal Fundus from fluorescein images", Med Image Anal. **12(2)**, 174-190 (2008)

[5] R. Ng, M. Levoy, M. Bredif, G. Duval, M. Horowitz, ´ and P. Hanrahan. Light field photography with a handheld plenoptic camera.

[6] R. Raskar, A. Agrawat, C. A. Wilson and A. Veeraraghavan. Glare Aware Photography: 4D Ray Sampling for Reducing Glare Effects of Camera Lenses, ACM Transactions on Graphics (TOG) 27 (3), 56.

[7] R. Ng, and P Hanrahan. Digital correction of Lens Aberrations in LightField Photography. In: International Optical Design, p. WB2, OSA

[8] A. R. Tumlinson and M. J. Everett. "Light field camera for fundus photography ", US8998411 B2

[9] M. Turola and S. Gruppetta, "4D Light Field Ophthalmoscope: a Study of Plenoptic Imaging of the Human Retina", Frontiers in Optics 2013/Laser Science XXIX, Volume: JW3A.36, 2013

[10] https://www.youtube.com/watch?v=riefZrlBa2s.

[11] FDA clinical trial database, https://clinicaltrials.gov/ct2/show/NCT03037268.

[12] M. Katz, "Introduction to Geometrical Optics", World Scientific, ISBN 981-238-202-X, 161

[13] O. Pomerantzeff, R H. Webb, and F.C. Delori, "Image Formation in Fundus Camers', Invest. Ophthalmol. Visual Sci, 18(6):630-7, (1979).

[14] M. Levoy and P. Hanrahana. "Light Field Rendering", Proc ACMSIGGRAPH (1996)

[15] http://www.zemax.com/os/resources/learn/knowledgebase/zemax-models-of-the-human-eye

[16] G. Wetzstein, Stanford EE 367 class notes, lecture 8, https://stanford.edu/class/ee367/